Comparative Study on Sodium Storage Properties of Two CNTs and a Novel CNT Design

[1,2]Tingting Xu, [1,2]Xiaohua Xie*, [2]Huisheng Huang** and [3]Xinwei Zhao

[1]*School of Environmental and Chemical Engineering, Three Gorges University, Chongqing 404120, PR China.*
[2]*Environmental School of Green and Intelligence, Yangtze Normal University, Chongqing 408100, PR China.*
[3]*Department of Physics, Tokyo University of Science, 1-3 Kagurazaka, Shinjuku-ku, Tokyo 162-8601, Japan.*

xiepingchang@163.com*; h.s.huang@hotmail.com**

(Received on 8th April 2022, accepted in revised form 6th February 2023)

Summary: Density functional theory (DFT) is employed to research three carbon tubes (CNTs), SWCNT, N-NiCNT, and N-CoCNT. The first two structures synthesized by other groups and N-NiCNT has better sodium storage properties as sodium-ion battery (SIB) anode than SWCNT, the last one is a designed structure. Here, the intrinsic cause why N-NiCNT has better performance than SWCNT has been located at molecular and atomic levels, meanwhile the potential of N-CoCNT as anode candidate is predicted. The researched properties that determine the electrochemical performances involve in structure stability, frontier molecular orbital, partial density of state analysis, and sodiation barrier comparison. The results indicate that the lower sodiation barrier, expanding transfer space, more stable structure stability of N-NiCNT should be responsible for its better sodium storage performance, which consists with the experimental results. In addition, the designed N-CoCNT anode is a promising candidate as SIB anode owing to better stability, lower barrier, and strong N-Co interaction than N-NiCNT.

Keywords: Carbon tube nanomaterials; Hard carbon; Carbon-based materials; DFT; Sodium ion batteries.

Introduction

The increasing requirement of power sources has given rise to essential development of energy storage devices. Lithium-ion batteries (LIBs) are the main power system of electronic products, yet the shortage of lithium resources restricts the mass application of LIBs [1-3]. Alternatively, sodium-ion batterie (SIB) as one of ideal choices for the next generation of large-scale energy storage technology has aroused extensive attentions in these years due to their low cost, inexhaustible natural sodium resources, and similar technology to LIBs [4-8].

Generally, SIBs mainly make up of positive electrode, negative electrode, electrolyte and current collector [8-10]. The anodes are mainly composed of carbon-based and non-carbon materials, and the later ones primarily consist of titanium-based materials, organic materials, alloy materials, metal oxides/sulfides. However, the capacity of titanium-based anode material is relatively low, the organic anode materials easily dissolve in the electrolyte, the alloy anodes tend to volume expansion after inserting sodium ions, and the metal oxides/sulfides are prone to reunions [11-13]. Thus, the above shortages limit the mass application of non-carbon anodes.

Carbon-based materials mainly refer to hard carbon materials, which are excellent candidates for anodes in SIBs owing to low potential, moderate capacity of sodium storage, small volume expansion, and excellent cycling performance. More recently, the exploration of hard carbon has opened the access of utilizing carbon-based anode for SIBs. In addition, numerous concerns have been poured on synthesizing different hard carbons and optimizing their electrochemical properties [14-16]. Currently, two types of precursors, polymers [17-18] and biomass materials, are commonly employed, but the formers are not widely used for manufacture due to high cost. In this regard, biomass-derived hard carbon anodes have been given more attention originating from their low cost, extensive resources, and stable electrochemical performances [19-20], and the first discharge-specific capacity reaches to 547.2 mAh/g at 100 mA/g [21]. According to our investigation, most of the biomass-derived hard carbons have been modified, and the modified hard carbons possess better electrochemical performance. In 2021, Chen *et al.* [22] synthesized hard carbons doped by nickel (Ni) and nitrogen (N), and the doped hard carbons obviously show better cycling performance benefitting from the ultrahigh solid-solid interface contact between

*To whom all correspondence should be addressed.

Ni and Na_2S. That same year, Liu *et al*. [23] compared sodium storage properties between pure hard carbon and hard carbon doped by Ni and N, and they found that the doped one showed better rate performance (Under 1200 mA/g current density, the discharge-specific capacity is 21 and 222.6 mAh/g for pure hard carbon and hard carbon doped by Ni/N, respectively.). How does Ni/N affect the sodium storage properties, and what is mechanism of the sodiation? [24-26]

For the sake of ascertaining the above questions and revealing out the properties that could not be obtained from experiment, the electronic structure and sodiated properties of two CNTs, SWCNT and N-NiCNT, are studied at molecular and atomic levels. In addition, a new CNT structure, N-CoCNT, is designed and researched to predict its potential as SIB anode. In the calculation, the edge of hard carbon structures is saturated by hydrogen atoms.

The contribution is arranged as follows. In Section 2, the main computational methods are explained. In Section 3, the Ni/N effects on hard carbons are analyzed, and Section 4 is the Conclusion.

Calculation Methods

In the contribution, DFT is carried out through employing the Dmol3 module of Materials Studio packages [27], with the exchange and correlation energy functional treated by the Perdew-Wang (PWC) functional of the local density approximation (LDA) [28]. The basis vector of the dual-value orbital basis set (DND) is implemented to describe the atomic orbital. The setting values of all models in the optimization process remain the same. The all-electron spin-unrestricted Kohn-Sham wave functions were expanded in a local atomic orbital basis. A convergence criterion of 10^{-5} au on the energy and electron density was performed for self-consistent field procedure, and the k point is set to 1×1×1. Besides, Na atom was added to the ground state of the structure that reached the most stable convergence standard and the total energy was calculated, as well as the electronic structure and properties.

In the work, the adsorption energy of different carbon nanotubes (CNTs) after adsorbing Na atoms was calculated as the following equation:

$$E_{ads} = E_{CNT+Na} - E_{CNT} - E_{Na} \qquad (1)$$

Here, E_{CNT+Na} is the total energy of the whole system after adsorbing Na, E_{CNT} is the total energy of unadsorbed CNTs (including doped CNTs), and the total energy of Na atom is E_{Na}.

Results and Discussions

CNT structures

CNT structure properties

In the work, the zigzag (8, 0) single-walled carbon nanotubes (SWCNT) are taken as research targets and the effects of adding N, Ni, Co atoms are investigated, as the CNT structures shown in Fig. 1. Fig. 1a is the undoped CNT structure, Fig. 1b is the N-Ni doped CNT structure in which the bonding N and Ni atoms replace one carbon atom, respectively, and the analogical design is as given in Fig. 1c. The cell parameters were set as 1×1×3 layers and a=20 Å, b=20 Å, c=25Å, α=β=γ=90º, respectively. The two edges of the studied CNTs are saturated with H atoms.

In order to analyze the doped effects on the CNT structures from N and heavy metals, the six-member cycles including N and heavy metals are selected as targets as C1-C2-C3-C4-C5-C6, C1-C2-C3-C4- Ni-N, and C1-C2-C3-C4 -Co-N cycles given in Fig 1. Meanwhile, the corresponding bond lengths are listed in Table-1. As the data in Table-1, all the C1-C2, C2-C3, C3-C4 bond lengths decrease after N and heavy metal insertion, which demonstrates that the incorporation of heteroatoms improves the electrons delocalizing the whole six-member cycles and enhancing conjugation of the six-member cycle. In other words, all the bonds in the six-member cycles strengthen.

On the behalf of analyzing the electronic structure property, the charges for the six-member cycles are studied in Fig. 2. In comparison of the charges for SWCNT and N-NiCNT in Fig. 2, the charge of C1 (0.002 for SWCNT and 0.176 for N-NiCNT) decreases (more positive) obviously, which originates from the strong electronegativity of doped N atom, while the charge of C4 (0.004 for SWCNT and -0.162 for N-NiCNT, respectively) increase (more negative) obviously, which is due to the strong ability of losing electron for doped Ni atom (0.379). In addition, the charge changes from SWCNT to N-NiCNT for both C2 (-0.001 for SWCNT, -0.047 for N-NiCNT) and C3 (0.004 for SWCNT, 0.002 for N-NiCNT) are small, respectively.

Table-1: The bond lengths of selected six-member cycles. (Å)

CNTs	C1-C2	C2-C3	C3-C4	C4-C5	C5-C6	C4-Ni	Ni-N	C4-Co	Co-N
SWCNT	1.54	1.54	1.54	1.54	1.54	-	-	-	-
N-NiCNT	1.44	1.46	1.41	-	-	1.80	1.86	-	-
N-CoCNT	1.45	1.47	1.41	-	-	-	-	1.84	1.87

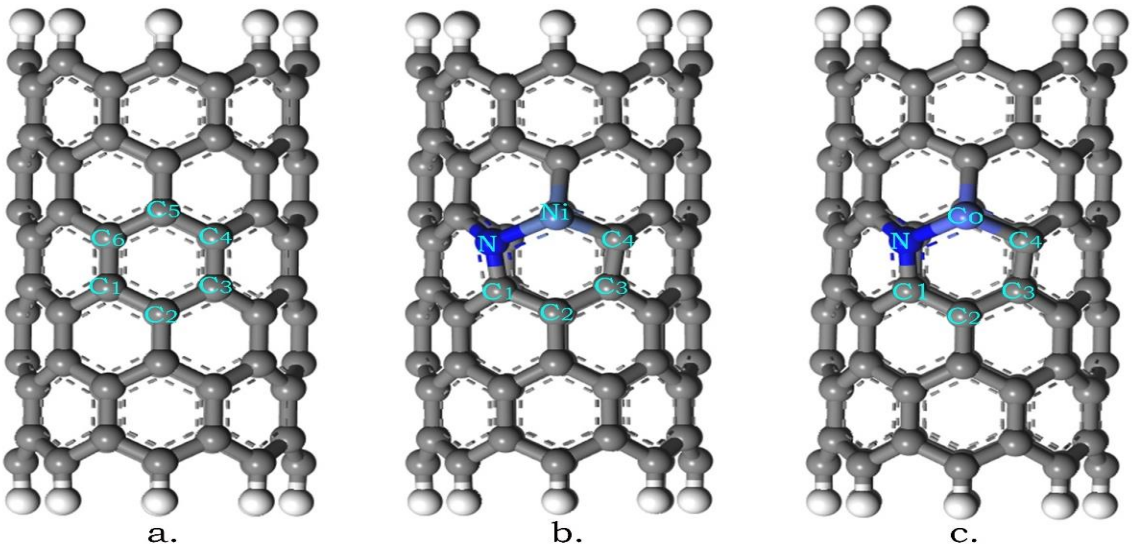

Fig. 1: The CNT structures of a) SWCNT, b) N-NiCNT, c) N-CoCNT.

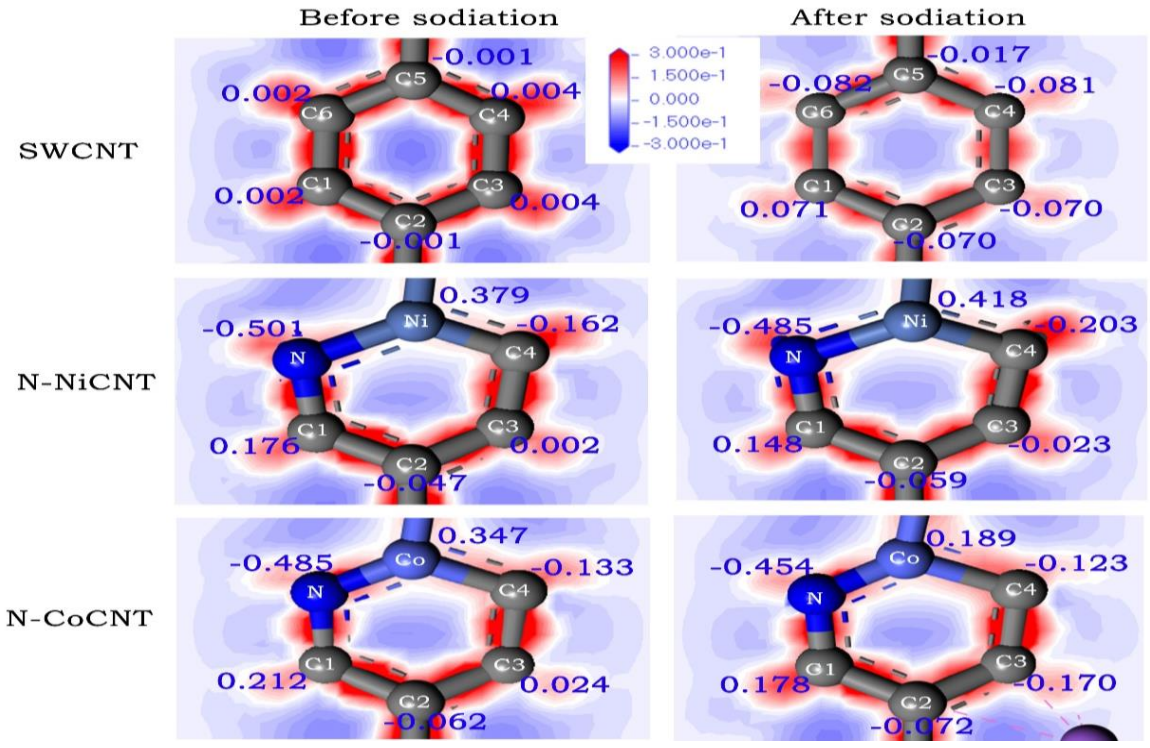

Fig. 2: The charges for the six-member cycles (the red field stands for positive charge and blue field stands for negative charge).

Furthermore, the charges of all the atoms for the selected six-member cycle in N-CoCNT are analogous to N-NiCNT, therefore, its electronic structure property is the same as N-NiCNT.

In a word, the N and Ni insertion strengthens the structural stability owing to electron delocalization, and the strong interactions are formed between the CNTs and Na atom. Furthermore, the designed N-CoCNT has the same structural stability as N-NiCNT and can form strong interactions with Na atoms as given in Fig. 2.

Frontier molecular orbital levels of CNTs

The frontier molecular orbital (*FMO*) levels consist of the highest occupied molecular orbital (*HOMO*) and the lowest unoccupied molecular orbital (*LUMO*), and the *FMO* levels affect the anode performance. Generally speaking, the FMO levels of SIB anodes should possess small energy gap (*Eg*), which benefits for both the electrolyte selection and the electron transfer in the charging and discharging process [29-30]. Thus, the *FMO* levels in the contribution are shown in Fig. 3.

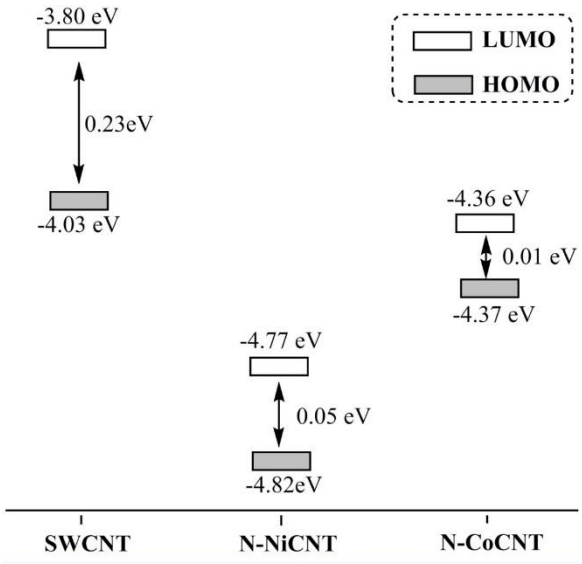

Fig. 3: The HOMO and LUMO levels of CNTs.

In comparison of the *FMO* levels in Fig. 3 we can see that the N and Ni insertion effectively decreases the *Eg* value (0.23 eV for SWCNT and 0.05 eV N-NiCNT, respectively), which is good for matching electrolyte due to less likely causing oxidation of electrolytes and electron transfer. What is notable is the designed anode material, N-CoCNT, which possesses narrower *Eg* than N-NiCNT and beneficial to selecting electrolyte and electron transfer. The atomic contributions of FMO are given in supporting information Fig. 1S.

CNT structures after sodiation

Structure analyses

In order to acquire the most stable sodiation position, the four kinds of sodiated CNTs are calculated, and the four sodiation sites which are defined as T, B, H, and Hin sites as depicted in Fig. 4. Here, T site is directly above the C atom on the outer wall of the tube (doped CNT is directly above the N atom), B site is directly above the midpoint of the C-C bond on the outer wall (doped CNTs are directly above the midpoint of N—Co, N—Ni, respectively), H site is directly above the center of mass of a six-membered carbon ring on the outer wall of the CNT (doped CNT is directly above the centroid of the doped six-membered ring), and Hin site is directly above the centroid of a six-membered carbon ring on the inner wall of the CNT (doped CNT is respectively directly above the centroid of the six-membered ring doped on the inner wall). The total energies of four sodiated structures are listed in Table-2. As the data in Table-2, both most stable sodiated site for both SWCNT and N-NiCNT is Hin site, while the H site is the most stable sodiated site for N-CoCNT. Besides, the vivid sodiated structures are given in Fig. 5(a, b, c). Notably, After sodiation for SWCNT and N-NiCNT, all the charges for the carbon atoms in the six-member cycle increase (more negative) as depicted in Fig. 2, which illustrates that the strong interactions are formed between the six-member cycle and Na atom.

Table-2: Total energies of studied CNTs at different positions after sodiation. (eV).

CNTs	B site	T site	H site	Hin site
SWCNT	-103302.78	-103302.72	-103302.94	-103303.38
N-NiCNT	-143739.47	-143739.44	-143739.41	-143739.79
N-CoCNT	-141172.00	-141172.00	-141172.08	---

Sodiation analyses

Since the sodiation ability of anodes plays an important role for SIB performance, the sodiation properties are researched in the paper. The sodiation energies of all the CNTs are given in Table-3, and the calculated basis is equation (1).

Table-3: The sodiation energies for different CNTs at different adsorption positions. (eV).

CNTs	B site	T site	H site	Hin site
SWCNT	35.23	35.24	35.04	34.62
N-NiCNT	-2.44	-2.43	-2.40	-2.70
N-CoCNT	-21.55	-21.56	-21.64	---

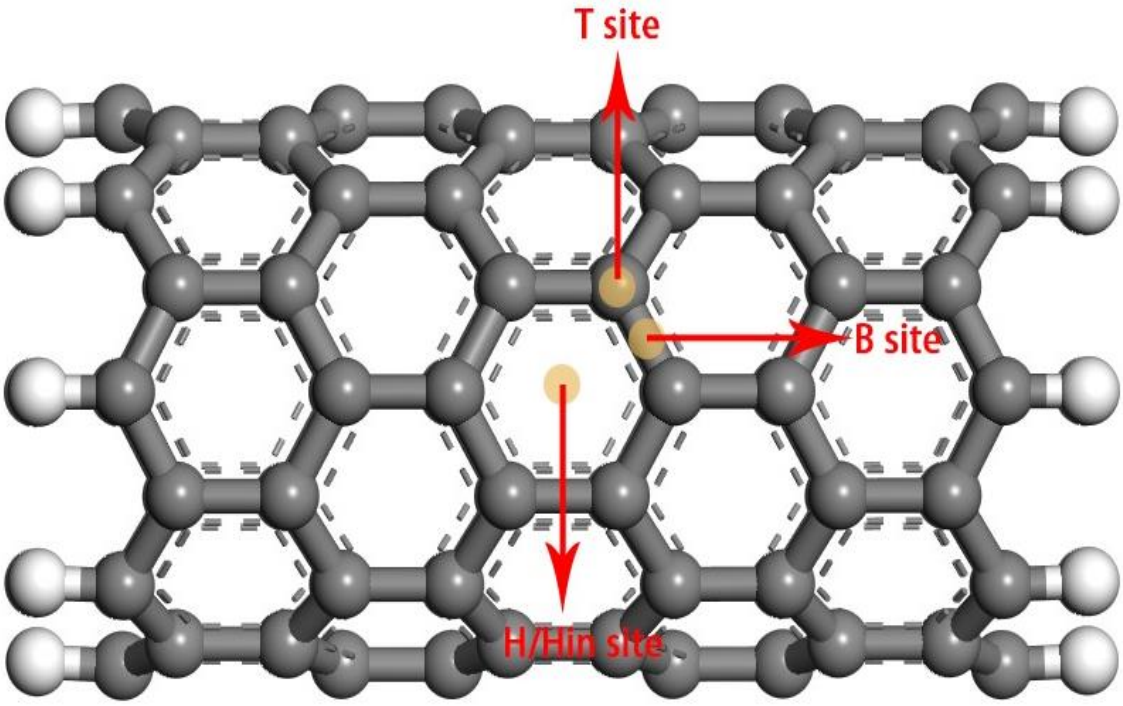

Fig. 4: The calculated adsorption position for CNTs.

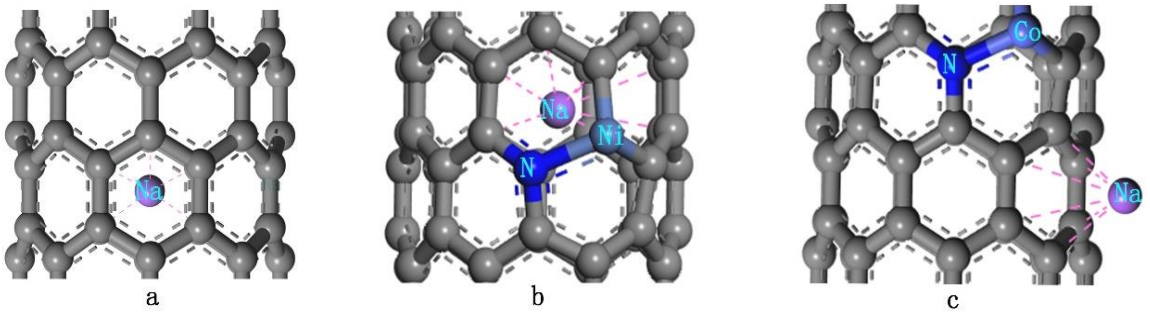

Fig. 5: The obtained best sodiated positions for a) SWCNT (Hin site), b) N-NiCNT (Hin site), and c) N-CoCNT (H site).

As the data in Table-3, all the sodiation energies for CNT at different adsorption position are around 35 eV, which suggests that the sodiation energy barrier of CNT is relatively high. However, the N and Ni insertion obviously decreases the sodiation energies for all the calculation sites (more negative, below -2.40 eV), which reduces sodiation barrier and promotes charging and discharging for SIB. Furthermore, the sodiation energies for designed anode N-CoCNT in all the sites (B site: -2.44 eV, T site: -2.43 eV, H site: -2.40 eV, and Hin site: -2.70 eV, respectively) are quite smaller than those of corresponding N-NiCNT (B site: -21.55 eV, T site: -21.56 eV, and H site: -21.64 eV, respectively), herein, Na will experience lower barrier in the sodiates process when is N-CoCNT as anode compared with N-NiCNT anode.

In comparison of the three CNT structures, Undoped CNT has the highest sodium intercalation barrier, followed by N-NiCNT and N-CoCNT, thus, the insertion of N and Ni decreases sodiation barrier and improves the SIB performance, and the designed anode N-CoCNT is a better candidate as SIB anode than N-NiCNT due to lower sodiation barrier.

Partial Density of state analyses

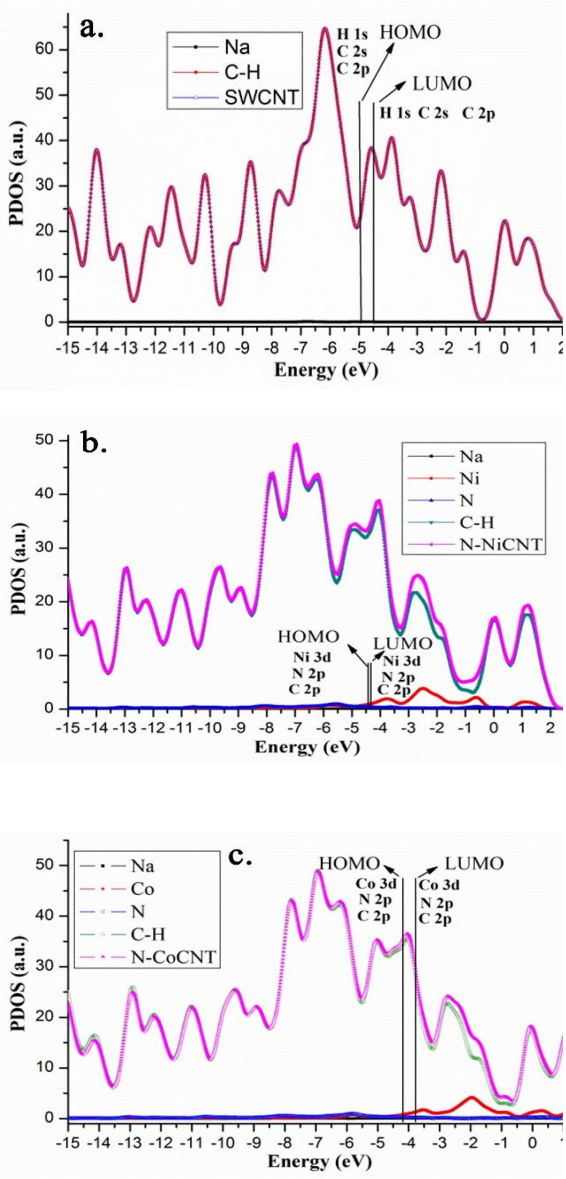

Fig. 6: The PDOS for studied CNTs after sodiation.

Partial density of state (DOS) is an effective analysis method for researching electron distribution in the orbitals. Thus, we analyze the PDOS properties depicted in Fig. 6, and the studied CNTs are divided into several parts, such as SWCNT is divided into two parts (Na and C-H) and N-NiCNT is divided into four parts (Na, C-H, N, Ni) as well as N-CoCNT (Na, C-H, N, Co).

As the Fig. 6a, the SWCNT (hollow upper triangle) is mainly contributed by C-H part (solid circle) and the Na part (solid square) makes little contribution to SWCNT. Further, the contributed atom orbitals mainly are from H 1s, C^{2s}, and C^{2p}. As for N-NiCNT in Fig. 6b, the N-NiCNT (solid left triangle) mainly consists of three segments, C-H (solid lower triangle, C^{2p} orbital), Ni (solid circle, 3d orbital), and N (solid upper triangle, 2p orbital), while Na (solid square) contributes little part. Therefore, the N-NiCNT PDOS shows that electrons distribute on N and Ni atoms, and the N^{2P} and Ni^{3d} orbitals play positive roles for forming stable N-Ni bond, which consists with the experimental results from XPS [31]. Analogously, as the N-CoCNT PDOS shown in Fig. 6c, the N-CoCNT (semi-hollow diamond) is mainly composed of C-H segment (hollow circle), Co (solid pentagram), and N (left hollow triangle), while Na segment does little contribution to the total DOS. In addition, the heavy metal Co^{3d} orbital and N^{2p} orbital keep strong interaction, which benefits to form strong N-Co bond and stable six-member conjugated cycle. As the mention of above analyses, the little contribution from Na to the total DOS mainly originates from the little electrons of outer layer, thus, the contribution degree is relative smaller comparing with other segments.

In order to locate all the roles of segments in SWCNT, N-NiCNT, and N-CoCNT, we calculate the PDOS of individual segments as given in Fig. 2S in supporting information. Here, we just analyze SWCNT. As the SWCNT-Na in Fig. 2S, the 3p and 3s atomic orbitals of Na contribute to the *HOMO* and *LUMO* of SWCNT, though the contribution is little (below 0.1). Meanwhile, the C^{2p}, C^{2s}, and H^{1s} from C-H segment contribute to the HOMO and LUMO in SWCNT.

Furthermore, the FMO levels and major contributor are emphasized on Fig. 6, and the HOMO and LUMO level are depicted with straight line, respectively. Besides, the detailed *FMO* levels and *Eg* values of CNTs after sodiation are given in Table 4. Through comparing Fig. 3 and Table-4 we can see that all the *FMO* levels have been changed after sodiation though Na contributes little on the FMO.

Table-4: The HOMO, LUMO, and energy gap (*Eg*) levels of studied CNTs after sodiation. (eV).

CNTs	HOMO	LUMO	*Eg*
SWCNT	-4.98	-4.74	0.24
N-NiCNT	-4.42	-4.39	0.50
N-CoCNT	-4.17	-3.86	0.31

In conclusion, N and Ni form stable chemical bonds after doping in CNT structures, and the N^{2p} and Ni^{3d} keep strong interactions, which benefits to form stable six-member cycles and decrease barrier for Na insertion.

Mechanism Analyses and Potential Prediction

Clarifying the mechanism of sodium embedding is helpful for the follow-up experimental research. Therefore, we analyze the mechanism of sodiation in studied CNTs.

The doping of N and Ni improves the electrochemical performance of CNTs both proved by experiment and theory, which may originate from the following causes. Firstly, the insertion of Na in the studied CNT systems meets the adsorption mechanism due to decreasing adsorption energy. Secondly, the other cause may be that the larger heteroatom provides larger space for Na. Thus, the sodiation mechanism in the studied CNT systems meets the adsorption-filling mechanism [32]

As to the designed N-CoCNT structure, it is a candidate for excellent anode due to its better stable six-member cycles and small barrier of Na transfer than N-NiCNT.

Conclusions

In the paper, DFT is carried out to locate the intrinsic causes why N-NiCNT has better sodium storage performance than undoped CNT. The electronic structures, frontier molecular orbitals, partial density of state, and sodiation barrier are investigated. The results indicate that the sodiation process meets the adsorption-filling mechanism and the insertion of N and Ni can effectively decrease barrier of Na transfer, provide larger space, and strengthen structure stability. Besides, The N^{2p} orbital and Ni^{3d} orbital interacts strongly, which consistent with the experimental results. In addition, the designed N-CoCNT anode possesses better stability, smaller barrier than N-NiCNT due to the strong N-Co inter action and is a promising candidate anode material.

Acknowledgements

This work was supported by Research Proje ct from Chongqing Committee of Education (Grant N o. KJQN202201429), Fuling Science and Technology Bureau Project (Grant No. FLKJ2021BBB2055), and Chongqing Municipal Education Commission (CXQ T20026).

References

1. R. Xu, G. Wang, T. Zhou, Q. Zhang, H.P. Cong, X. Sen, J. Rao, C.F. Zhang, Rational design of Si@carbon with robust hierarchically porous custard-apple-like structure to boost lithium storage, *Nano Energy.,* **39**, 253 (2017)
2. L. Yu, L.P. Wang, H. Liao, Z. Feng, Understanding Fundamentals and Reaction Mechanisms of Electrode Materials for Na-Ion Batteries,*Small.,* **14,** 1703338. (2018)
3. M. Wahid, D. Puthusseri, Y. Gawli, N. Sharma, S. Ogale, Hard Carbons for Sodium-Ion Battery Anodes: Synthetic Strategies, Material Properties, and Storage Mechanisms, *ChemSusChem.,* **11,** 506 (2018)
4. Y. Zhang, Y. Huang, V. Srot, A. Peter, J. Maier, Y. Yu, Enhanced Pseudo-Capacitive Contributions to High-Performance Sodium Storage in TiO2/C Nanofibers via Double Effects of Sulfur Modification, *Nano-Micro Letters*., **12,** 165 (2020)
5. X. Xue, D. Sun, X. Zeng, X. Huang, H. Zhang, Y. Tang, H. Wang, Two-step carbon modification of NaTi2(PO4)3 with improved sodium storage performance for Na-ion batteries, *Journal of Central South University.*, **25**, 2320 (2018)
6. L. Fan, S. Wei, S. Li, Q. Li, Y. Lu, Recent Progress of the Solid-State Electrolytes for High-Energy Metal-Based Batteries, *Advanced Energy Materials.,* **8,** 1702657 (2018)
7. M. Murayama, X. Xie, S. Guan, X. Zhao, A review on research progress in electrolytes for sodium-ion batteries, *SCIENTIA SINICA Technologica.*, **50**, 247 (2020)
8. J. Hwang, S. Myung, Y. Sun, Sodium-ion batteries: present and future, *Chemical Society Reviews*., **46,** 3529 (2017)
9. R. Jia, G. Shen, D. Chen, Recent progress and future prospects of sodium-ion capacitors, *Science China Materials.*, **63**, 185 (2020)
10. R. Usiskin, Y. Lu, J. Popovic, M. Law, P. Balaya. Y. Hu, J. Maier, Fundamentals, status and promise of sodium-based batteries, *Nature Reviews Materials.,* **6**,1020 (2021)
11. H. Kim, H. Kim, Z. Ding, M. Li, K. Lim, G. Yoon, K. Kang, Recent progress in electrode materials for sodium-ion batteries, *Advanced Energy Materials.,* **6,**1600943 (2016)
12. H. Pan, Y. Hu, L. Chen, Room-temperature stationary sodium-ion batteries for large-scale electric energy storage, *Energy & Environmental Science.*, **6**, 2338 (2013)
13. Q. Wang, C. Zhao, Y. Lu, B. Zhang, Advanced nanostructured anode materials for sodium-ion batteries, *Small.,* **13**, 1701835 (2017)

14. Y. Li, Y. Yuan, Y. Bai, Y. Liu, Z. Wang, L. Li, F. Wu, K. Amine, C. Wu, Insights into the Na+ storage mechanism of phosphorus-functionalized hard carbon as ultrahigh capacity anodes, *Advanced Energy Materials.,* **8,** 1702781 (2018)
15. L. El. Moctar, Q. Ni, C. Wu, F. Wu, Hard carbon anode materials for sodium-ion batteries, *Functional Materials Letters.,* **11,** 1830003 (2018)
16. F. Wu, M. Zhang, Y. Bai, X. Wang, R. Dong, C. Wu,Lotus seedpod-derived hard carbon with hierarchical porous structure as stable anode for sodium-ion batteries, *ACS Applied Materials & Interfaces*., **11,** 12554 (2019)
17. Y. Bai, Z. Wang, C. Wu, R. Xu, F. Wu, Y. Liu, H. Li, J. Lu, J. Lu, K. Amine, Hard carbon originated from polyvinyl chloride nanofibers as high-performance anode material for Na-ion battery, *ACS Applied Materials & Interfaces.,* **7**,5598 (2015).
18. F. Wu, R. Dong, Y. Bai, Y. Li, G. Chen, Z. Wang, C. Wu, Phosphorus-doped hard carbon nanofibers prepared by electrospinning as an anode in sodium-ion batteries, *ACS Applied Materials & Interfaces.,* **10,** 21335 (2018)
19. X. Lin, Y. Liu, H. Tan, B. Zhang, Advanced lignin-derived hard carbon for Na-ion batteries and a comparison with Li and K ion storage, *Carbon.,* **157,**316 (2021)
20. B. Zhang, C.M. Ghimbeu, C. Laberty, C. Vix-Guterl, J.M. Tarascon, Correlation Between Microstructure and Na Storage Behavior in Hard Carbon, *Advanced Energy Materials.*, **6**, 1501588 (2016)
21. M. Liu, Y. Huang, C. Chen, Cedarwood bard-derived hard carbon as anode for high performance sodium-ion batteries, *Energy Fuels.*, **34,** 11489 (2020)
22. K. Song, J. Liu, H. Dai, Y. Zhao, S. Sun, J. Zhang, C. Qin, P. Yan, Atomically dispersed Ni induced by ultrahigh N-doped carbon enables stable sodium storage, *Chem.,* **7,** 2684 (2021)
23. T. Liu, H. Ye, J. Li, Synthesis and sodium storage performance of the nickel metal and nitrogen element co-doped carbon nanotube materials, *Journal of Chinese Electron Microscopy Society.,* **40,** 228 (2021)
24. Y. Zhang, X. Li, P. Dong, G. Wu, J. Xiao, X.Y. Zeng, Y. Zhang, X. Sun, Honeycomb-like hard carbon derived from pine pollen as high-performance anode material for sodium-ion battery, *ACS Applied Materials and Interfaces.,***10**, 42796 (2018)
25. O.I. Malyi, T. L. Tan, S. Manzhos, A Comparative Computational Study of Structures, Diffusion, and Dopant Interactions between Li and Na Insertion into Si, *IOP SCIENCE*.,6, 027301 (2013)
26. Y. Li, M. Chen, B. Liu, Y. Zhang, X.Q. Liang, X.H. Xiu, Heteroatom Doping: An Effective Way to Boost Sodium Ion Storage, Adv. Energy Mater., 10, 2000927 (2020)
27. P. V. vramo, K. N. Kudin, and G. E. Scuseria, Single wall carbon nanotubes density of states：comparison of experiment and theory, *Chemical Physics Letters.,* **370,** 597 (2003).
28. J.P. Perdew, and Y. Wang, Accurate and simple analytic representation of the electron-gas correlation energy, *Physical Review B.,* **45,** 13244 (1992).
29. J. Yang, Y. Wang, X. Zhou, L. Weng, Y. Liu, Y. Ren, C. Zhao, M. Dahbi, J. Alami, D. Abd Ei-Hady, G. Xu, K. Amine, M. Shao, and X. Liu, Electrolytes Polymerization-Induced Cathode-Electrolyte-Interphase for High Voltage Lithium-Ion Batteries, *Advanced Energy Materials.*, **11,** 2101956 (2021).
30. N. Karimi, M. Zarrabeitia, A. Mariani, D. Gatti, A. Varzi, Nonfluorinated Ionic Liquid Electrolytes for Lithium Metal Batteries: Ionic Conduction, Electrochemistry, and Interphase Formation, *Advanced Energy Materials.,* **11**, 2003521 (2021)
31. K. Song, J. Liu, H. Dai, Y. Zhao, S. Sun, J. Zhang, C. Qin, P.Yan, C. Wang, Atomically dispersed Ni induced by ultrahigh N-doped carbon enables stable sodium storage, Cell Press.,14, 2684 (2021)
32. P. Bai, Y. He, X. Zou, X. Zhao, P. Xiong, and Y. Xu, Elucidation of the sodium-storage mechanism in hard carbons, Advanced Energy Materials, 8, 1703217 (2018).